Applied Catalysis A: General 365 (2009) 199–206

Contents lists available at ScienceDirect

Applied Catalysis A: General

journal homepage: www.elsevier.com/locate/apcata

Catalyst testing in a multiple-parallel, gas–liquid, powder-packed bed microreactor

Daniël van Herk [a,1], Pedro Castaño [a], Michiel Makkee [a,*], Jacob A. Moulijn [a], Michiel T. Kreutzer [b]

[a] Catalysis Engineering, Faculty of Applied Sciences, Delft University of Technology, Julianalaan 136, 2628 BL Delft, The Netherlands
[b] Product and Process Engineering, Faculty of Applied Sciences, Delft University of Technology, Julianalaan 136, 2628 BL Delft, The Netherlands

ARTICLE INFO

Article history:
Received 14 April 2009
Received in revised form 7 June 2009
Accepted 8 June 2009
Available online 17 June 2009

Keywords:
Hydrogenation
High-throughput experimentation
Trickle bed
Packing

ABSTRACT

The use of a three-phase plug-flow microreactor with powder catalysts to obtain intrinsic kinetics is reported. Our test reaction is the hydrogenation of biphenyl over a Pt-Pd/Al_2O_3 catalyst. We compare reaction rates obtained in both our microreactor and a standard hydrogenation autoclave. The reactor design consists of six parallel reactor tubes with an inner diameter of 2.2 mm and a maximum catalyst-bed length of 200 mm.

Co-flowing two phases very slowly over the bed needs more care than running only a liquid or a gas. Our main contribution in this work is to stress the impact of hydrodynamic anomalies, most importantly stagnant zones of gas and liquid, which occurred in reactor columns where diluent and catalyst were unevenly distributed. Such packing irregularities caused huge variations in conversion levels from tube to tube. In contrast, using a proper way to load the solids evenly, we could get the same results in each reactor tube. The values of these kinetic constants were identical to the ones we obtained in the autoclave. The well-known effect that too much dilution causes loss of conversion is found to be stronger than that in gas–solid systems. We visualized flow patterns in a 2-dimensional reactor mock-up and found such stagnant zones in segregated beds. Scaling down a continuous packed-bed reactor to reliably measure catalytic kinetics for gas–liquid–solid reactions is possible under specified conditions described herein.

1. Introduction

Whereas the scaling-up of reactors is seen to be a task of considerable complexity, the opposite task of scaling down is often heralded as the panacea to chemical reactor ills [e.g. 1,2]. This paper argues that for catalyst testing this is a too simplistic view, especially for the multiphase reactors that are considered here. Indeed, in miniaturized reactors most temperature and concentration gradients vanish due to the faster transport at reduced scale. This cannot be said, however, for the flow behaviour. Small does not automatically exclude maldistribution and incomplete wetting. The careful analysis of these effects is the main contribution of this work. For an overview of scaling aspects in general, the reader is referred to references [3,4].

For catalysis, the development cycle begins with a broad screening of thousands of samples (the discovery phase, stage 1), followed by a detailed investigation of the best candidates (the optimization phase, stage 2). In the first stage, "quick-and-dirty" analysis that allows different candidates to be ranked suffices. This stage has benefited significantly [5–7] from advances in the robotics and the fabrication techniques [e.g. 8]. In stage-1 testing one can sometimes avoid multiphase operation by choosing a suitable gas-phase-only model reaction. In the second stage – which we are interested in this paper – experiments must yield accurate data of kinetics and deactivation for process design. Here, the developments have been more gradual, and the existing equipment has been optimized rather than replaced. As a result, Mills and Nicole [9] have argued that the second stage is now often the bottleneck in industrial catalyst development.

Miniaturized, automated, parallel reactor systems have been used for decades in catalysis and are still being actively developed, both in academia [10–14] and in industry [15–17]. Classically, in the case of gas–liquid–solid systems, kinetic tests are either performed in autoclaves [13,18] with fresh catalysts in powder form or in fixed-bed reactors with diluted shaped catalysts [13].

While the continuous fixed bed systems have the distinct advantage of showing catalyst performance over longer time, Hickman et al. [19] have argued that incomplete wetting and associated external mass transfer limitations can "completely dominate" the kinetics under investigation. To overcome this issue,

* Corresponding author. Tel.: +31 15 278 1391; fax: +31 15 278 5006.
E-mail address: m.makkee@tudelft.nl (M. Makkee).
URL: http://www.dct.tudelft.nl/ce
[1] Current address: HTE Aktiengesellschaft, Kurpfalzring 104, 69123 Heidelberg, Germany.

0926-860X/$ – see front matter © 2009 Elsevier B.V. All rights reserved.
doi:10.1016/j.apcata.2009.06.010

Nomenclature

a	dimensionless deactivation constant in Eq. (3)
d_p	particle diameter, m
F	mass flow rate of biphenyl, $g_{BPh}\ h^{-1}$
$k(t)$	reaction-rate constant, $g_{BPh}\ h^{-1}\ g_{cat}^{-1}$
L	catalyst bed length, m
n	reaction order
Pe_p	particle Péclet number
r	dilution ratio, $ml_{diluent}\ ml_{cat}^{-1}$
t	time, s
W	mass of catalyst inside the reactor, g_{cat}
$X(t)$	conversion as a function of time

Greek letters

λ	deactivation parameter in Eq. (3)
ρ_p	particle density, $kg\ m^{-3}$

their suggestion was to operate such a reactor in recycle at high superficial velocities that ensured good wetting. They used full-sized catalyst pellets with or without 70 μm diluent in a 10 mm reactor at typically 5 mm s^{-1} liquid flow velocities.

Motivated by the same need for full wetting, Bej et al. [20,21] explored the effect of diluent size on shaped catalyst performance. Briefly, their finding was that complete wetting could be achieved in fixed-bed reactors (13 mm id) at liquid velocities below 0.1 mm s^{-1}, but only when the diluent was smaller than 200 μm. At larger diluent size, considerable variation in conversion occurred at these space velocities. An alternative approach is to avoid diluents altogether. Normally, this leads to significant liquid maldistribution, a problem that Kallinikos and Papayannakos circumvented by packing a string of shaped particles in a tight-fitting column, ensuring good wetting by operating in up-flow [22,23]. Within experimental error, this device reproduced the conversion levels of a large-scale reactor.

The objective of the current work is to develop a fixed-bed test to evaluate long-term performance of powder catalysts, such that it gives the reliable rates that are – initially, for the fresh catalyst – the same as those obtained in an autoclave over the whole range of conversion. Our interest in such a test comes from the desire to study the reaction rate and its decline over time without any diffusion limitations inside the catalyst. The most pressing question, in our view, is whether proper catalyst wetting and contacting can be achieved in a reactor without recycles. Eventually, the goal is to perform these tests at high-conversion levels, to avoid the extrapolation of differential reactor behaviour to integral reactor behaviour.

In previous studies, we investigated various hydrodynamic aspects such as axial dispersion and hold-up in homogeneously packed systems [24,25], and here we explicitly ask ourselves what happens when the particles are not uniform in size and density. We are most interested in the flow pattern at low velocities and we report dedicated visualization experiments, both in a uniform homogeneous bed and in a segregated one. Our most important result is that the diluent needs to be carefully matched to the catalyst powder to obtain a bed without any segregation. A diluent is still desired in powder packed beds, not so much to enhance wetting, but rather to increase bed length for plug flow conditions [4]. A common-used criterion for the bed length L to ensure axial dispersion is [26]:

$$L > 20n\frac{d_p}{Pe_p}\ln(1-X) \quad (1)$$

where X is the conversion, d_p is the particle diameter, and Pe_p is the particle Péclet number. To ensure this bed length, in related work [27] we found that the catalyst-loading procedure is as crucial here as it is for larger particles [28].

Berger et al. [29] investigated powder-catalyst dilution in a gas–solid system, from which a model was formulated that represented the deviation of the conversion due to the dilution:

$$X_{diluted} = \left(\frac{d_p r}{2L} + \frac{1}{X_{undiluted}}\right)^{-1} \quad (2)$$

where r is the dilution ratio, i.e. the volume of the diluent and catalyst combined divided by the volume of the catalyst. $X_{diluted}$ and $X_{undiluted}$ are the conversion of the diluted bed and of the undiluted bed, respectively.

The paper is organized as follows: after discussion of several design aspects of the reactor set-up and the experimental procedures, we report repeated performance tests that we compare with our experiments in a stirred autoclave, for which we can exclude transport phenomena affecting the kinetics. We analyze the reproducibility, or lack thereof, in terms of visually observed features of the flow.

2. Experimental

2.1. Set-up

The set-up consists of 6 parallel continuous reactors. The reactors have an inner diameter of 2.2 mm and a packed-bed length of 475 mm. The heated part of the reactor consists of coincidentally 6 vertically aligned insulated brass blocks with a heating wire helically coiled around the perimeter. Each block is independently maintained at set-point temperature with a master–slave control loop. The inner 3 blocks (no. 3–5 from the top) are isothermal within 0.5 °C, as was verified in each reactor tube. The catalyst-bed length in this isothermal zone is at least 200 mm. Flow rates of gas (pure hydrogen) are between 5 and 50 ml min^{-1} (STP) and those of liquid are between 0.5 and 5 g h^{-1}.

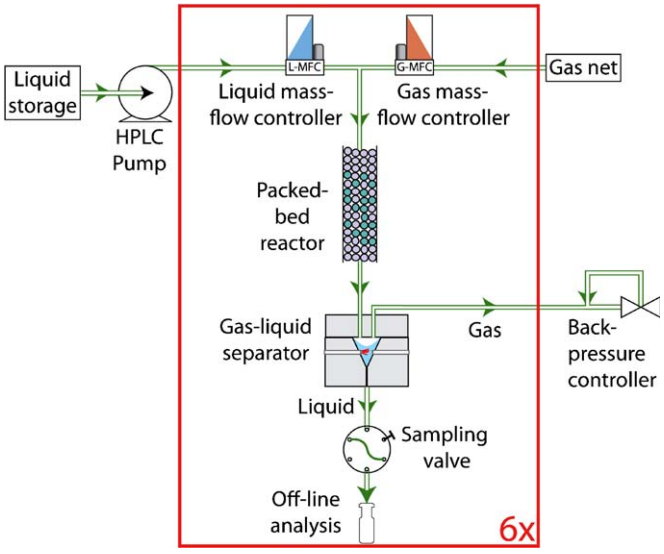

Fig. 1. A schematic overview of equipment components. The part encapsulated by the box is present in six-fold. Gas and liquid are fed continuously to the reactor tubes (d = 2.2 mm, L = 500 mm), such that the reactors operate at independent space velocity. The reactors are filled with ~0.1 mm particles. All reactor tubes are maintained at the same temperature. The gas leaves through a back-pressure controller, keeping all reactors are at the same pressure. The liquid is removed semi-continuously using a sampling valve and collected for off-line analysis.

The set-up is designed to withstand a maximum pressure of 10 MPa and a reactor temperature of up to 500 °C.

In Fig. 1 a schematic overview is given. The effluent of each reactor runs into a gas–liquid separator. The gas effluent of these separators are merged and vented through a vessel that is maintained at constant pressure with a bleed inflow from mass-flow controller and a combined outflow through a back-pressure controller, such that equal pressure is guaranteed in all reactors. The liquid effluent is semi-continuously removed using a six-way valve and a sample loop. Samples of this liquid flow are directed to a fraction collector and, subsequently, analyzed off-line.

The two top requirements for the gas–liquid separator are high-pressure resistance and a small internal volume. With respect to the latter, it should be noted that each millilitre of dead space corresponds to up to an hour of residence time and, as a consequence, sampling delay. We have designed and built a funnel with level control that fulfils these requirements. At two different levels at the bottom end of the funnel, the phase is detected with an infrared signal and detector. Fig. 2(a) shows a schematic drawing of the gas–liquid separator. The evolution of the collected light in time during filling and emptying of the funnel is shown in Fig. 2(b).

2.2. Materials

The particles used consist of bimetallic catalyst on alumina (purchased from Hereaus, Hanau, Germany): 0.1 wt.% Pt, 0.4 wt.% Pd/Al_2O_3. The catalyst is crushed and sieved in the ranges 53–90 μm, 90–150 μm, and 150–250 μm. The different fractions are denoted by the approximate mean values 70, 120, and 200 μm. The inert, nonporous particles used are silicon carbide (Cats, Rotterdam, The Netherlands), supplied in the (mean) sizes 40, 100, 150, and 180 μm. In one case also non-porous glasses beads are used as inert, which are sieved in the range 45–63 μm (denoted by 55 μm).

The liquid feed consists of a tetradecane (Acros, Geel, Belgium, 99%) solution with 8.4×10^{-2} mol l^{-1} (~2 wt.%) of biphenyl (Acros, 98%) as a reactant and 4.4×10^{-2} mol l^{-1} of hexadecane (Merck, Hohenbrunn, Germany, 99%) as an internal standard for the gas chromatograph. The feedstock in this work is desulphurized with an adsorbent (Ni-NiO/Al_2O_3 from BASF, De Meern, The Netherlands) [see 30, for details]. Typical values of the sulphur content before and after desulphurisation are 638 ± 12 and 19.4 ± 0.1 ppb, respectively.

2.3. Operating procedure

Weighed amounts of catalyst powder and diluent powder were premixed and introduced at once into a funnel that feeds into a reactor tube. Each reactor was loaded in three steps: bottom inert, the catalyst–inert mixture, and finally a layer inert on top. The bed height for an undiluted bed was almost 7 mm, and for a twenty-fold dilution by volume with SiC, the bed height was about 150 mm. In most cases the dilution with SiC was four-fold by volume, resulting in a bed length of about 35 mm. After the first filling step and during the third filling step, the reactor tubes were tapped to compact the bed. After filling, the reactor tubes were mounted leak-tight in the set-up. Details of the optimum packing procedure are given in [27]. The catalyst was reduced *in situ* by a continuous flow of hydrogen (30 ml min^{-1}) at 250 °C at atmospheric pressure, in 4 h. After reduction, the system was cooled down, pressurized and the gas flow was allowed to stabilize. Subsequently, the temperature was raised, and then the liquid flow was set. The experiments were generally performed at a pressure

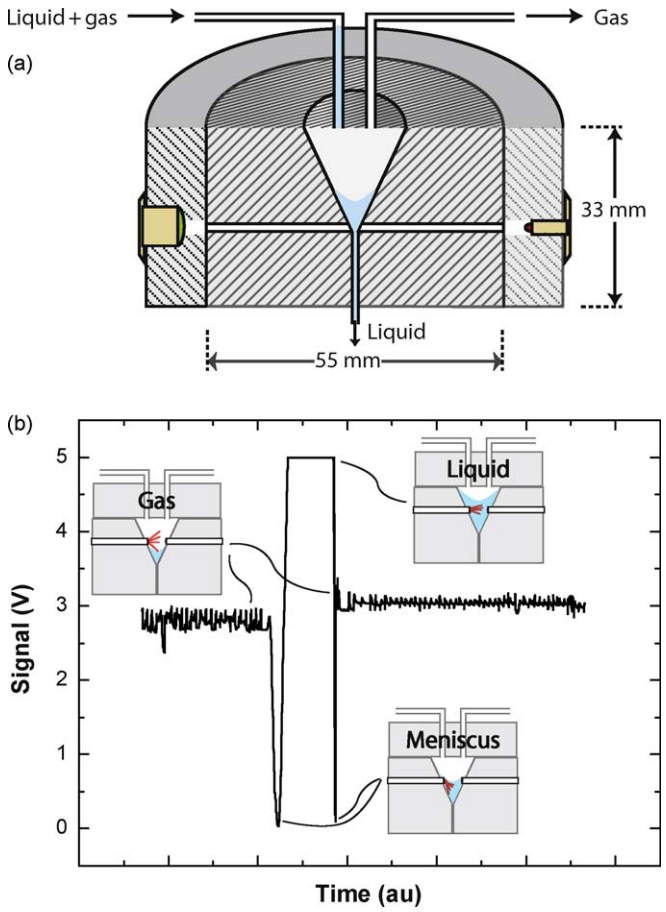

Fig. 2. The gas–liquid separator: (a) a schematic cutaway view of the gas–liquid separator. The fluid phase that is present in the path of the IR beam is detected by the amount of transmitted light. (b) The signal indicating the amount of light passing through the gas–liquid separator recorded during filling and emptying. The cartoons indicate the light path at the different liquid levels.

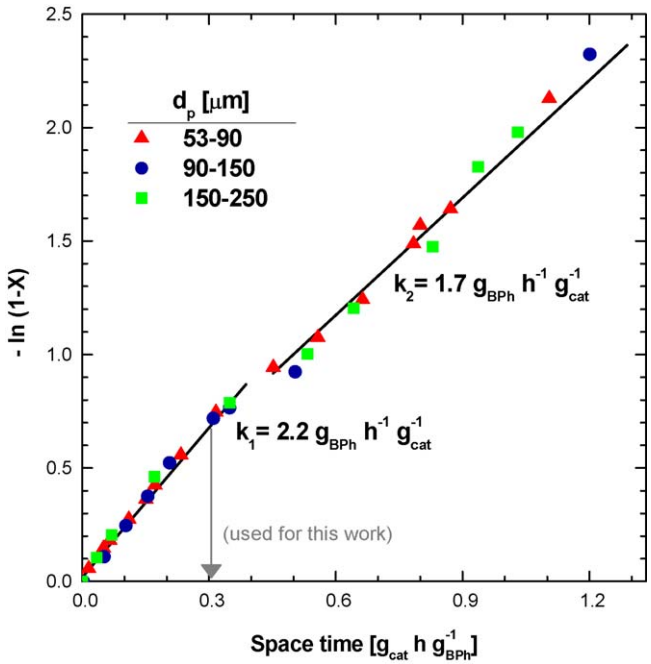

Fig. 3. Conversion versus space-time in autoclave experiments using particles of different sizes, indicating the absence of diffusion limitation inside the particles. *Conditions*: T = 140 °C, p = 5 MPa, 1 g of catalyst in 150 ml feed with $C_{BPh,0}$ ~2 wt.%.

of 5 MPa and temperature of 140 °C. During experiments, samples were taken at selected time intervals. Each sample was preceded by a 'waste sample' to flush the lines towards the sample vial. At a typical flow rate of the liquid, 4 g h^{-1}, one sample was taken every 15 min. The analysis was performed off-line in a gas chromatograph (Chrompack CP9001, 50 m HP-1 column, FID detector).

2.4. Data processing

The initial conversion level $X(0)$ for a fresh catalyst was determined by fitting values of $X(0)$ and λ in the most appropriate deactivation function [30],

$$a = \frac{X(t)}{X(0)} = \frac{1}{1+\lambda t} \quad (3)$$

to the $X(t)$ measurements in each interval of isothermal operation. The reaction rate constant $k(t)$ was obtained from $X(t)$:

$$k(t) = -\frac{F}{W}\ln[1 - X(t)] \quad (4)$$

where F is the mass-flow rate of biphenyl into the reactor and W is the catalyst mass inside the reactor. In the case of irreproducible results, modelling does not make sense and, therefore, both the resulting value and the error are not representative, as mentioned with the data.

The autoclave data were taken from ref. [30].

2.5. Visualisation experiments

Visualisation experiments were performed in 2-dimensionally patterned polydimethyl-siloxane (PDMS) chips. The chips were manufactured using standard soft-lithographic techniques [31]. The measurements were performed in the same day as molding and bonding in order to have reliable wetting properties of the PDMS [32]. The PDMS chips contained regular arrays of hexagonally positioned pillars. Pillars of two diameters were fabricated, 100 and 150 μm, respectively. The center-to-center distance was 1.5 times the pillar diameter. The PDMS channel was 5.5 mm wide, 55.0 mm long, and 70 μm deep. Ethanol, having similar wetting and viscosity at room conditions as tetradecane at reaction conditions, was fed to the device by a syringe pump (Harvard PHD2000). Airflow to the device was regulated with a needle valve (Porter, VCD-1000). Rhodamine-B was used as fluorescent dye to enhance contrast.

The flow was visualized with an inverted epifluorescent microscope (Zeiss axiovert 200 M) equipped with a CCD camera (La Vision, Imager Intense). Images were recorded at frame rates of 2 or 4 Hz with an exposure time of 5 ms. A series of these images, typically consisting of 240–960 images or about 2–8 min, are processed to obtain a space-resolved value for the time-average liquid fraction in the bed. The flow rates were 0.4 and 4.0 mm s^{-1} for the liquid and gas phase, respectively. These velocities are the same as those typically applied in the microreactor.

3. Results

3.1. Comparison of autoclave and packed-bed

Fig. 3 shows the pseudo-first order kinetics of the reaction, obtained in autoclave experiments with particles of different size. The reaction-rate constant at 140 °C was determined to be $k = 2.2 \pm 0.2$ g_{BPh} h^{-1} g_{cat}^{-1} and the activation energy was found to be $E_A = 94 \pm 11$ kJ mol^{-1} (from runs at different temperatures, see ref. [30]). No decrease in reaction rate was observed for particle sizes up to 200 μm. We used a pseudo-first order kinetic model instead of a Langmuir–Hinshelwood model, because at the low reactant concentrations employed here, the simpler model was sufficiently

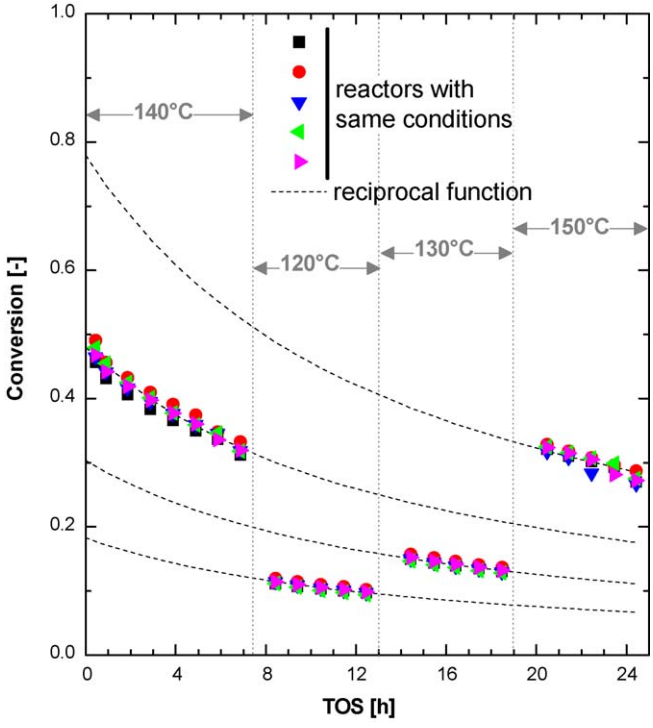

Fig. 4. Reproducibility of the catalyst performance, shown in conversion versus time on stream (TOS), in five parallel reactors. These experiments were performed with an optimal combination of catalyst size and diluent size. During the experiments the temperature is varied as indicated. The dotted lines captures the deactivation behaviour, using the reciprocal model for remaining fractional activity $a = (1 + \lambda \cdot TOS)^{-1}$, as described by Castaño et al. [30]. *Conditions*: p = 5 MPa, superficial liquid velocity = 0.4 mm s^{-1}, space-time = 0.32 g_{cat} h g_{BPh}^{-1}. Catalyst: W = 23.4 mg (0.029 ml), d_p = 70 μm. Diluent: SiC, 200 mg (0.129 ml), d_p = 100 μm.

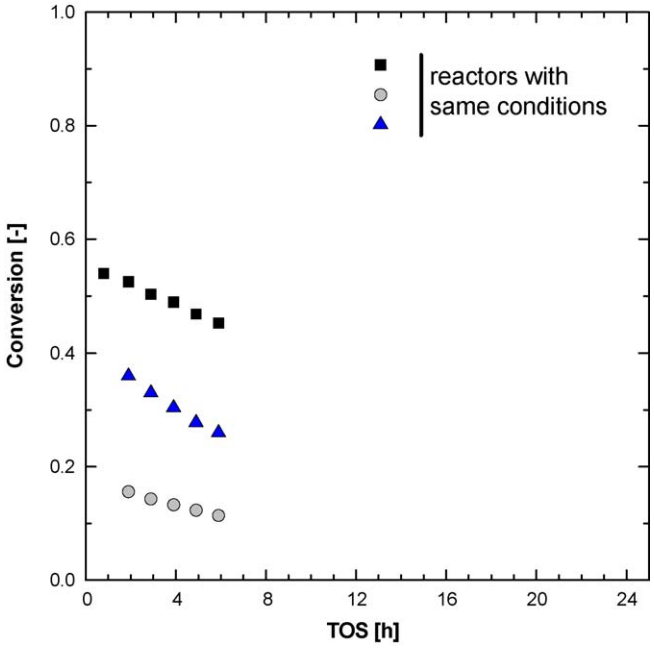

Fig. 5. Irreproducible conversion levels obtained simultaneously in 3 different reactors. The relevant difference with the reproducible runs, as shown in Fig. 4, is the different diluent size. *Conditions*: p = 5 MPa, superficial liquid velocity = 0.4 mm s^{-1}, space-time = 0.31 g_{cat} h g_{BPh}^{-1}. W = 23.2 mg (0.028 ml), d_p = 70 μm. Diluent, SiC, 400 mg (0.258 ml), d_p = 180 μm.

adequate to describe the relation between conversion and space-time in the autoclave experiments.

We now compare the conversion in the autoclave with conversion in the continuous reactors. For a space-time of 0.316 g_{cat} h g_{BPh}^{-1} the conversion in the autoclave was 0.501 ± 0.007. The initial conversion in 5 reactors at the same space-time, in Fig. 4, was 0.472 ± 0.016. The difference between the two reactor types is 6%.

3.2. Reproducibility

The reproducibility of the conversion in the microreactors was investigated by operating several reactors at the same flow rate of gas and liquid simultaneously and comparing their performance. Because all reactors drew liquid from the same batch of reactant, the amount and composition of the deactivating poisons in the feed were identical for all reactors. The reactors were packed with the same batch of diluent and catalyst. The construction of the set-up ensured that all reactors operated at the same pressure and temperature. These observations serve to emphasize that variations in performance are due to the reactor packing, not due to variations in reactants or operating conditions.

We account for small experimental variations as follows. Each column is connected to two mass flow controllers, one for gas flow and one for liquid flow. We determined that random deviations from set-point of the mass flow controllers were ~2% of full scale. The error in the amount of catalyst in each reactor was less than 1%. The error in temperature was ~0.3 °C. Using E_A = 94 kJ mol^{-1} from [30], the combined propagation of these experimental errors in the error of the conversion is 3% or less.

This error analysis invites comparison to the experimental error reported in Fig. 4. The experimental error was 3%, comparable to the theoretical prediction. In other words, the packing of the reactors (method optimized before [27]) did not introduce any significant variation in performance.

The reproducibility reported in Fig. 4 shows the result of our efforts to optimize the loading and operation of these reactors. We discuss this optimization later in detail, but first, we show that at suboptimal conditions, very significant variations in conversion occured. Fig. 5 shows very significant variations from reactor to reactor. For the space velocity in this experiment, the expected initial conversion based on the autoclave kinetics was 0.501 ± 0.007. In only one of the three reactors, the initial conversion was comparable to that value; in the other two reactors, the conversion is close to 0.4 and 0.2, respectively.

Fig. 6 offers a more condensed overview of reproducibility, in a column plot with error bars indicating the standard deviation, with each reactor indicating a different size of the diluent. For all the experiments in Fig. 6, the catalyst was the same. Clearly, the different diluents exhibit different amounts of systematic and random error.

Using the smaller diluents (40 μm SiC and 55 μm glass) reduced the average conversion level. For two combinations of catalyst size/diluent size (70 μm catalyst with 100 μm SiC, and 70 μm catalyst with 150 μm SiC), the reaction rate constant that was obtained from the continuous flow reactors agreed within experimental error with the kinetics obtained in the autoclave experiments. Using a larger diluent (180 μm SiC particles) resulted in a large variation in conversion, similar to that obtained in Fig. 5 for 100 μm SiC diluent with 120 μm catalyst particles.

As can be seen in Figs. 5 and 6, by using particles of SiC-180 μm it is possible (though not reproducible) to obtain a higher activity than predicted by the autoclave experiments. We have observed that this combination of catalyst and SiC can lead to a segregated

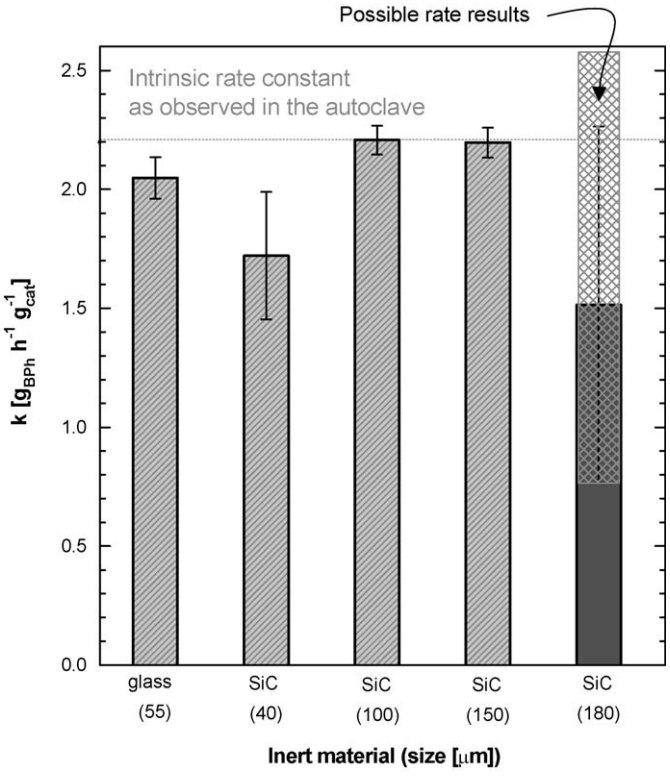

Fig. 6. The reaction rate constants, observed for fresh catalyst using different diluent sizes and materials, and the reproducibility (both in parallel and in different runs) as indicated by the error bars. The dotted line shows that rate constant that was measured in an autoclave at identical conditions (Fig. 3). The results for 180 μm SiC are not reproducible and, therefore, the model used to find the initial rate constant is not optimal, so the values here are estimated based on the trend in Fig. 5. *Conditions*: p = 5 MPa, superficial liquid velocity = 0.4 mm s^{-1}, space-time = 0.31 g_{cat} h g_{BPh}^{-1}. Catalyst: W = 24 mg (0.03 ml), d_p = 70 μm. Diluent: SiC, 200 mg (0.129 ml), d_p = 100 μm. Diluent, glass, 200 mg (0.112 ml), d_p = 50 μm.

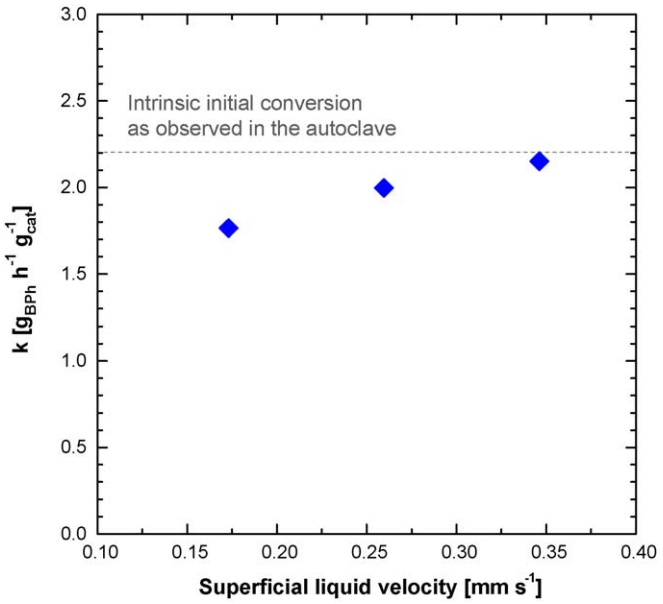

Fig. 7. Initial reaction-rate constant, measured (in one experiment with 3 parallel reactors) at varying liquid flow rates while keeping the space velocity constant, indicating that mass transfer outside the particles is not measurably influencing the catalyst performance above 0.35 mm s^{-1}. The effect of flow rate shows even less correlation at other temperatures (not shown here). *Conditions*: p = 5 MPa, space-time = 0.30 g_{cat} h g_{BPh}^{-1}. Catalyst: W = 10–20 mg (0.013–0.026 ml), d_p = 70 μm. Diluent: SiC, 80–160 mg (0.052–0.104 ml), d_p = 100 μm.

bed [27] with a compact reaction zone with a reduced area for heat exchange, such that hot spots can be generated. A hypothetical adiabatic reactor would have a conversion level of 60.5%, or k_{obs} = 2.58 g_{BPh} h^{-1} $g_{cat}{}^{-1}$, for the conditions presented here, to be compared with the isothermal conversion of 50.1% (k = 2.2 g_{BPh} h^{-1} $g_{cat}{}^{-1}$). The rates reported in Fig. 6 are within a range confined by the adiabatic case, and a possible explanation for the somewhat higher conversion levels is a slight temperature rise in completely undiluted and/or highly segregated beds.

Fig. 6 also includes the very reproducible experiment shown in Fig. 4, with 70 μm catalyst and 100 μm SiC diluent, as well as another experiment (70 μm catalyst with 150 μm SiC) that was equally reproducible. In summary, both the size of the catalyst and the size of the diluent are important parameters to obtain reproducible results.

3.3. Effect of flow rate

The external mass-transfer limitation was investigated by variation of the catalyst loading while keeping the space-time constant. Because intrinsic kinetics depend only on space-time and should be independent of flow velocity, this is a convenient direct method to check for mass transfer limitations. The results are shown in Fig. 7. We repeated these experiments at other temperatures (not shown in Fig. 7) that show even less dependence of conversion on flow rates. If any, little influence is observed for a liquid velocity higher than 0.35 mm s^{-1}: at higher flow rates the rate constant is within the experimental error.

3.4. Effect of dilution ratio

Experiments spanning a wide range of dilution ratio (from 0 to 20 units diluent volume per unit catalyst volume) were used to explore the effect of high dilution rates on conversion. The results are presented in Fig. 8. Although the undiluted bed shows an average conversion value in agreement with the reference experiments (0.477 versus 0.501), the error in conversion for the undiluted bed (0.047) is higher than that predicted by the error propagation analysis (experimentally 10% versus predicted 3% relative error). A likely explanation for this increased experimental error is that the undiluted bed is very shallow, only 7 mm high, such that thermal exchange with the isothermal surrounding was insufficient to prevent a small temperature rise. The heat exchange in such a small bed is irreproducible: the bed is too short to statistically average out local packing variations.

Adding a small amount of diluent, with a volumetric dilution ratio of less than 5, does significantly reduce the experimental error and also does not lower the conversion extensively. In contrast, at dilution ratios higher than 10, the conversion decreases drastically. We observe a linear trend of conversion versus dilution ratio, resulting in a five-fold reduction of conversion at a dilution ratio of 20 (v/v).

3.5. Visual observation of flow patterns

A first attempt to explain the very strong impact of diluent size and catalyst size was performed in the 2D microfabricated beds, which offered a glimpse at what happens in these powder beds at low velocities. Fig. 9 shows time-averaged liquid-fractions for two beds; in other words, even irrigation of these structures would result in a homogeneous even grey level in these images. Very light areas are predominantly filled with gas, and very dark areas are predominantly filled with liquid. The flow in Fig. 9 is from left to right.

The right-hand side of Fig. 9 shows the equivalent of a homogeneous bed: all the pillars are of the same size. The irrigation

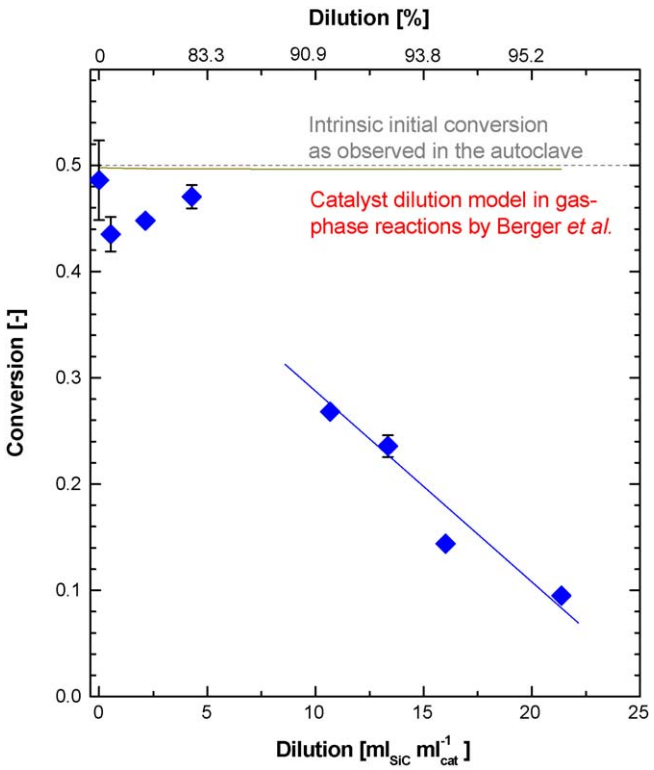

Fig. 8. The initial conversion (corrected for the variation in catalyst amount) versus catalyst-to-inert dilution ratio measured in several runs. The error bars represent the standard deviation in the conversion of the experiments that have been repeated. By keeping the dilution between 1:1 and 1:5 volumetric ratio, the resulting conversion is within the kinetic regime. At lower ratios, the results are irreproducible, at higher ratios, the conversion is lower. *Conditions*: p = 5 MPa, superficial liquid velocity = 0.4 mm s^{-1}, space-time = 0.31 g_{cat} h $g_{BPh}{}^{-1}$. W = 23.1 mg (0.029 ml), d_p = 70 μm. Diluent, SiC, 0–1000 mg (0–0.52 ml), d_p = 100 μm.

of these pillars is very even as well, as is evident from the grey levels in the time-averaged map. This indicates that it is indeed possible to evenly irrigate a bed that is packed with powders—at least when all the particles have the same size.

The left-hand side of Fig. 9 shows a very different irrigation. In this structure, zones of pillars of 100 μm were embedded in zones with pillars of 150 μm. This 50 μm difference in size is comparable to the size differences that caused problems in the continuous reactors. In regions where the relatively small micro-pillars (100 μm) were present, the liquid hold-up was higher (~95% versus ~85% of the void volume). As a result, the gas flow had a preference towards the large-pillar regions. A large portion of the small-pillar region never held any gas, and only rarely did we observe a channel of gas through these small-pillar regions.

In some chips, imperfections due to the microfabrication process removed one or two pillars in the bed. Such imperfections, which are the equivalent of large void pockets in a packed bed, induced a dynamic oscillatory flow which in a time-averaged sense, made the irrigation more even.

In summary, in a segregated bed with small and large pillars, the gas preferentially runs through the large pillars, and in a regular bed with mono-dispersed pillars, the gas flow follows a path through the bed more randomly.

4. Discussion

The results presented in Fig. 4 show that the performance of the catalyst in the autoclave can be reproduced in the fixed-bed microreactor: (i) accurately, with a deviation of 6% from intrinsic kinetic values and (ii) reproducibly, with a deviation of 3% from a

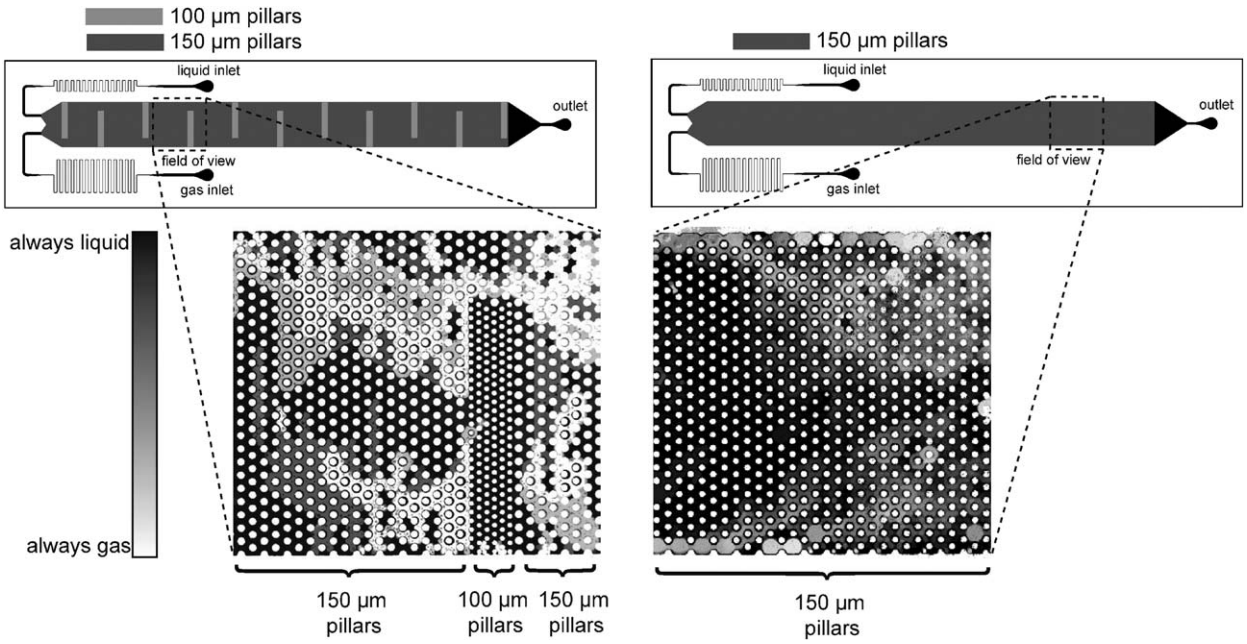

Fig. 9. Visual analysis of the impact of segregation on the flow in micropacked beds. The left chip design represents a maldistributed bed: it features a hexagonal array of pillars, mostly 150 µm pillars with several zones filled with smaller pillars of 100 µm diameter. The small-pillar zones were positioned such that fluids could flow around them. The micrograph shows the time-averaged liquid level (recording period 2–4 min) in a portion of the chip that was in the field of view of the microscope. The white holes in the image are the pillars themselves. The zone with small particles is fully filled with liquid at all time, without any gas passing through it. In contrast, the area that is filled with large pillars has several light-grey and dark-grey areas, indicating that gas passes through these zones. The right chip design has a homogeneous array of 150 µm pillars and the time-averaged micrograph shows less occurrence of fully wet or fully dry zones, which is ascribed to the presence of voids in the region before the captured section. *Conditions*: superficial liquid velocity = 0.4 mm s^{-1}, superficial gas velocity = 4 mm s^{-1}.

multiple parallel run. The total error that we found between different runs, separated by several days and with different batches of feed was 9%. All these values are about the same order as that of the error analysis and comparable to the error of 6.5% to 9% that is found from other reports of reproducibility data from a variety of different types of multiple parallel devices [33–36].

An intriguing observation is the strong effect of diluent size on the reproducibility. We must rule out diffusional limitations on a particle level, because the autoclave experiments with different particle size clearly showed the absence of internal transport limitations. The experiments at increasing flow rate rule out that a "film" around the particle forms a significant resistance to mass transfer, because such a film resistance would decrease with increasing flow rate. These conclusions are in agreement with the classical criteria used in catalyst performance testing [37].

The visual experiments provide an important clue: if segregation occurs for particles of different size, then the voids between the smaller particles remain liquid-filled and gas does not penetrate these pockets. For the liquid velocities used in this work (all the visualization experiments were done with 0.4 mm s^{-1}) the movement of the gas–liquid interface is dominated by the Laplace pressure jump across the interface (a good introductory reference for the analysis of such flows in porous media, very similar to this application in packed beds is [38]). In zones with small particles, a gas–liquid interface must make more jumps through smaller throats in comparison with a zone with larger particles. A gas bubble will follow the path of least resistance, which in many cases will be far from the small particles.

In other words, the wetting efficiency does not so much depend on the particle size in itself, but on the extent of segregation and the difference in particle size between catalyst and diluent. It is interesting to observe from the microfabricated pillar beds, that even rather small differences in pillar diameter already prevent access of gas to large zones inside the bed.

Our filling procedure, in which the catalysts fall a significant distance from the funnel, should depend strongly on the free-fall velocity of the particles that leave the funnel into the reactor tube: faster particles will end up near the bottom. It follows from Stokes' law for the friction of a falling sphere that the term $\rho_p \cdot d_p^2$ (with ρ_p and d_p as the particle density and diameter, respectively) is the relevant group that determines the free-fall velocity. As a result, segregation will be minimal if the free-fall velocity of the diluent and the catalyst are close to one another [27]. This can explain our experimentally observed reproducibility for catalyst particles of 70 µm in combination with diluents of 100–150 µm, because they have almost the same free-fall velocity. In contrast, 180 µm diluents fall much more rapidly during filling, probably resulting in segregation and surely resulting in varying conversion levels. It should be noted that tapping is much less effective in homogenizing a bed when the particles are small. Detailed investigations of the extent of segregation are described elsewhere [27].

A direct effect of an axially segregated bed is that the catalyst bed length is shorter, in the worst case as short as an undiluted bed. Using Eq. (1) with a particle Péclet value of 0.1 [24], at 0.5 conversion, the minimum bed length should be almost 10 mm. In such a case, small differences in the bed packing may have a significant effect on the bed length and on thermal exchange, which both affect the observed kinetics. The undiluted bed is less than 7 mm long, which can, therefore, explain low reproducibility (Fig. 8).

The low reproducibility observed in the beds with 180 µm SiC (Fig. 6) is also ascribed to the too short bed, which is now cause by segregation during loading: most of the diluent ends up in the bottom, and most of the catalyst ends up in a small section on top. Axial dispersion in short beds can explain lower conversion levels, and poor thermal exchange can generate hot-spots in a short bed. These phenomena combined may explain the occasional higher conversion measured (see error bars) in both undiluted beds (Fig. 8) and segregated beds (SiC = 180 µm in Fig. 6).

A second surprising observation is that dilution has such a profound impact on conversion level. We have tried to correlate the loss in conversion with the dilution ratio using the Berger model (Eq. (2)), which assumes a random radial walk of reactants in a bed of randomly distributed catalyst particles. For high dilution ratios, we found much higher loss of conversion, indicating that a non-random phenomenon must be in play. Perhaps an extensive shielding of catalyst particles by the surrounding diluents cause liquid to "non-randomly walk" past the catalyst. Alternatively, the catalyst particles can be non-randomly distributed in the bed, for instance mostly near the wall or mostly in the center. Combined with hydrodynamic wall effects, this could explain the strong influence.

We believe that multiphase operation leads to stable preferential paths that are strongly related to the local pore topology and associated interfacial pressure jumps: the packing configuration has a profound effect on the hydrodynamics. All the results in this paper lead to the conclusion that dilution only helps in achieving better defined, reproducible conditions when the diluent size is chosen with care, and extensive dilution always leads to extreme bypassing.

5. Conclusions

- We have reported a parallel, automated, miniaturized reactor system for performance testing of powdered catalysts in three-phase systems. Using a fast model reaction with significant deactivation, we obtain: (i) kinetic data ($X = 0.472 \pm 0.016$) that deviates 6% from autoclave experiments ($X = 0.501 \pm 0.007$); and (ii) reproducible results within a multiple parallel run, having a relative error in the conversion of ~3%, or ~9% for consecutive runs. The optimal conditions fur such reproducible and intrinsic results are: liquid flow rate higher than 0.35 mm s^{-1}, catalyst:inert dilution ratio of 1:4, catalyst:inert sizes of 70:100 or 70:150 μm.
- It is advisable in this multiple-parallel, gas–liquid microreactor to use always one of the reactor tubes with a reference catalyst for checking reproducibility.
- The reactor set-up was designed and constructed in-house. One important component was the gas–liquid separator that was specifically designed in order to meet the requirements of high pressure and low dead volume.
- Image analysis of flows in microfabricated beds, observed under a microscope, reveals that segregation of diluent and catalyst leads to preferential pathways in the bed, where the zones with the smallest particles are filled with stagnant liquid that is much less often refreshed than the gas and liquid lumps that travel through the larger particles.
- We found that conversion levels vary significantly in segregated beds. This could indicate that the extent of stagnant pockets formation, with associated mass transfer limitations on a scale of the order of the bed width, varies from reactor to reactor.
- When segregation is prevented – in our case this required matching the fall velocity of diluent and catalyst during packing – then the initial conversion level and the deactivation rate are reproducible within experimental error as mentioned above.
- Dilution reduces axial dispersion, but high dilution (a catalyst:inert dilution ratio above 1:4) reduces conversion significantly. The deviation is larger than one that is based on random walk of reactants, indicating that the isolated catalyst particles are shielded from the flowing reactants, either by radial segregation or by local shielding on a particle scale. Dilution should be done carefully; a volume ratio below 5 is optimal.

Acknowledgements

Massimiliano Quaglia is gratefully acknowledged for taking part in some of the experimental work. The authors thank Shell Global Solutions and Albemarle Catalysts Company for financial support.

References

[1] N. Yoswathananont, K. Nitta, Y. Nishiuchi, M. Sato, Chem. Commun. (2005) 40–42.
[2] S. Tadepalli, R. Halder, A. Lawal, Chem. Eng. Sci. 62 (2007) 2663–2678.
[3] D. Janasek, J. Franzke, A. Manz, Nature 442 (2006) 374–380.
[4] S.T. Sie, Rev. Instrum. Fr. Pét 46 (1991) 501–515.
[5] S. Senkan, Angew. Chem. Int. Ed. 40 (2001) 312–329.
[6] R.J. Hendershot, C.M. Snively, J. Lauterbach, Chem. Eur. J. 11 (2005) 806–814.
[7] D. Farrusseng, Surf. Sci. Rep. 63 (11) (2008) 487–513.
[8] M.W. Losey, R.J. Jackman, S.L. Firebaugh, M.A. Schmidt, K.F. Jensen, J. Microelectromech. Syst. 11 (2002) 709–717.
[9] P.L. Mills, J.F. Nicole, Ind. Eng. Chem. Res. 44 (2005) 6435–6452.
[10] R. Thomas, J.A. Moulijn, V.H.J. Debeer, J. Medema, J. Mol. Catal. 8 (1980) 161–174.
[11] J. Perez-Ramirez, R.J. Berger, G. Mul, F. Kapteijn, J.A. Moulijn, Catal. Today 60 (2000) 93–109.
[12] J.A. Moulijn, J. Perez-Ramirez, R.J. Berger, G. Hamminga, G. Mul, F. Kapteijn, Catal. Today 81 (2003) 457–471.
[13] A. Corma, J.M. Serra, Catal. Today 107–08 (2005) 3–11.
[14] G. Morra, D. Farrusseng, E. Guillon, S. Morin, C. Bouchy, P. Duchene, C. Mirodatos, Catal. Today 137 (2008) 71–79.
[15] W.H. Weinberg, B. Jandeleit, K. Self, H. Turner, Curr. Opin. Solid State Mater. Sci. 3 (1998) 104–110.
[16] J. Klein, W. Stichert, W. Strehlau, A. Brenner, D. Demuth, S.A. Schunk, H. Hibst, S. Storck, Catal. Today 81 (2003) 329–335.
[17] E. Maxwell, P. van den Brink, R.S. Downing, A.H. Sijpkes, S. Gomez, T. Maschmeyer, Top. Catal. 24 (2003) 125–135.
[18] S. Thomson, C. Hoffmann, S. Ruthe, H.W. Schmidt, F. Schuth, Appl. Catal. A 220 (2001) 253–264.
[19] D.A. Hickman, M. Weidenbach, D.P. Friedhoff, Chem. Eng. Sci. 59 (2004) 5425–5430.
[20] S.K. Bej, R.P. Dabral, P.C. Gupta, K.K. Mittal, G.S. Sen, V.K. Kapoor, A.K. Dalai, Energy Fuels 14 (2000) 701–705.
[21] S.K. Bej, A.K. Dalai, S.K. Maity, Catal. Today 64 (2001) 333–345.
[22] L.E. Kallinikos, N.G. Papayannakos, Ind. Eng. Chem. Res. 46 (2007) 5531–5535.
[23] L.E. Kallinikos, N.G. Papayannakos, Chem. Eng. Sci. 62 (2007) 5979–5988.
[24] D. van Herk, M.T. Kreutzer, M. Makkee, J.A. Moulijn, Catal. Today 106 (2005) 227–232.
[25] N. Márquez, P. Castaño, M. Makkee, J.A. Moulijn, M.T. Kreutzer, Chem. Eng. Technol. 31 (2008) 1130–1139.
[26] D.E. Mears, Chem. Eng. Sci. 26 (1971) 1361.
[27] D. van Herk, P. Castaño, M. Quaglia, M.T. Kreutzer, M. Makkee, J.A. Moulijn, Appl. Catal. A. accepted for publication (doi:10.1016/j.apcata.2009.06.003).
[28] M.H. Al-Dahhan, Y.X. Wu, M.P. Duduković, Ind. Eng. Chem. Res. 34 (1995) 741–747.
[29] R.J. Berger, J. Perez-Ramirez, F. Kapteijn, J.A. Moulijn, Chem. Eng. Sci. 57 (2002) 4921–4932.
[30] P. Castaño, D. van Herk, M.T. Kreutzer, J.A. Moulijn, M. Makkee, Appl. Catal. B 88 (2009) 213–223.
[31] G.M. Whitesides, A.D. Stroock, Phys. Today 54 (2001) 42–48.
[32] V. Berejnov, N. Djilali, D. Sinton, Lab Chip 8 (2008) 689–693.
[33] C. Hoffmann, H.W. Schmidt, F. Schuth, J. Catal. 198 (2001) 348–354.
[34] C. de Bellefon, N. Pestre, T. Lamouille, P. Grenouillet, V. Hessel, Adv. Synth. Catal. 345 (2003) 190–193.
[35] P. Mäki-Arvela, K. Eränen, K. Alho, T. Salmi, D.Y. Murzin, Top. Catal. 45 (2007) 223–227.
[36] G. Morra, A. Desmartin-Chomel, C. Daniel, U. Ravon, D. Farrusseng, R. Cowan, A. Krusche, C. Mirodatos, Chem. Eng. J. 138 (2008) 379–388.
[37] F. Kapteijn, J. Moulijn, in: G. Ertl, H. Knözinger, F. Schüth, J. Weitkamp (Eds.), Handbook of Heterogeneous Catalysis, 2nd ed., Wiley-VCH, Weinheim, 2008, pp. 2019–2045.
[38] R. Lenormand, E. Touboul, C. Zarcone, J. Fluid Mech. 189 (1988) 165–187.